Supporting Information

Pharmacophore Modeling and Virtual Screening for Novel Acidic Inhibitors of Microsomal Prostaglandin E_2 Synthase-1 (mPGES-1)

Birgit Waltenberger, Katja Wiechmann, Julia Bauer, Patrick Markt, Stefan M. Noha, Gerhard Wolber, Judith M. Rollinger, Oliver Werz, Daniela Schuster, Hermann Stuppner

Table of contents:

Chart S1. 72 confirmed inactive compounds of the mPGES-1 inhibitor test set

Chart S2. Compounds from the NCI database mapping all six pharmacophore model features that were selected for biological testing

Chart S3. Compounds from the Specs database mapping all six pharmacophore model features that were selected for biological testing

Chart S4. Compounds from the NCI database leaving out one pharmacophore model feature that were selected for biological testing

Chart S5. Structure of the 5-LO control inhibitor **S98** (BWA4C)

Figure S1. Viability of Jurkat A3 and A549 cells

Molecular docking of mPGES-1 inhibitors:

Figure S2. Compounds used for validation of docking run

Table S1. Glide-scores for compounds of docking run

Figure S3. Plot of glide-scores against pIC_{50}-values of ligands

Chart S1. 72 confirmed inactive compounds of the mPGES-1 inhibitor test set. [1-8] The compounds are sorted by increasing molecular weight. None of the molecules matched the restrictive pharmacophore model. Twelve compounds fitted the partial query pharmacophore model.

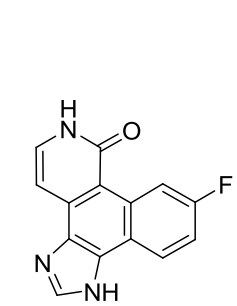
S1

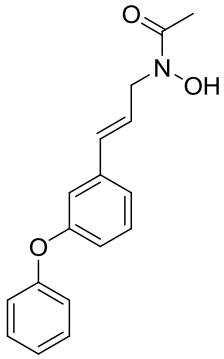
S2

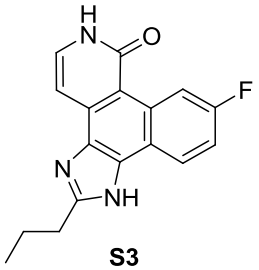
S3

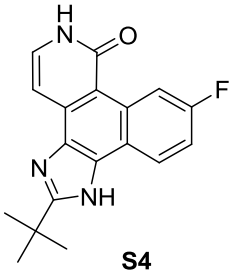
S4

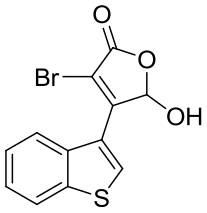
S5

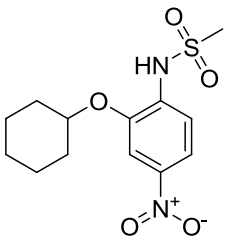
S6

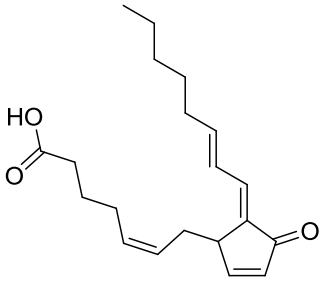
S7

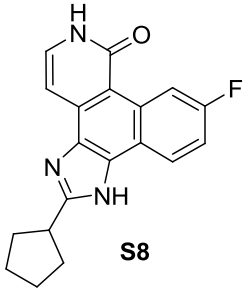
S8

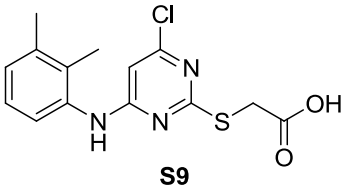
S9

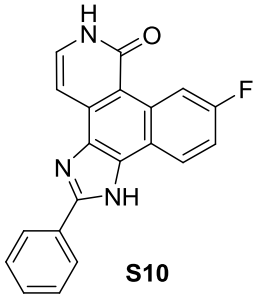
S10

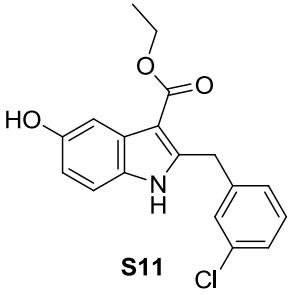
S11

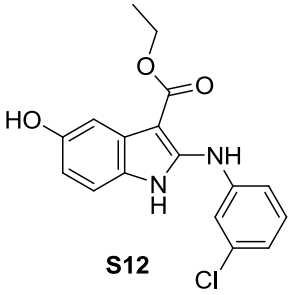
S12

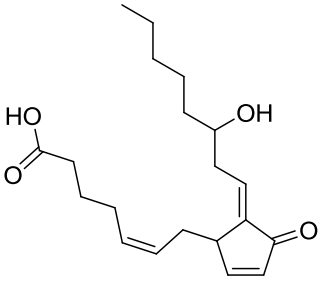
S13

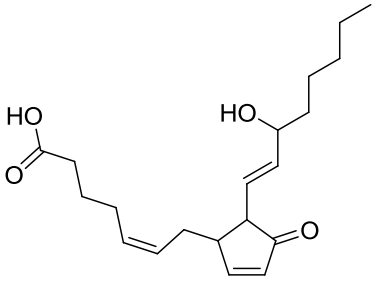
S14

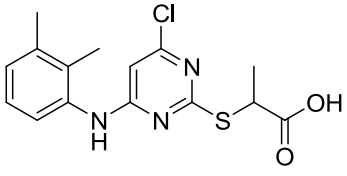
S15

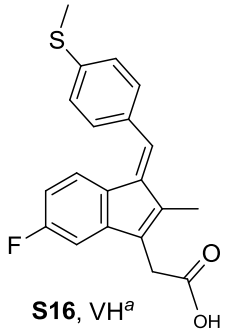
S16, VH[a]

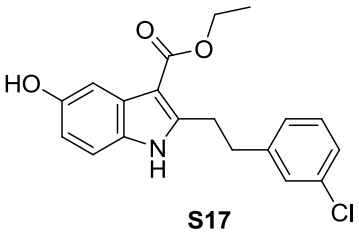
S17

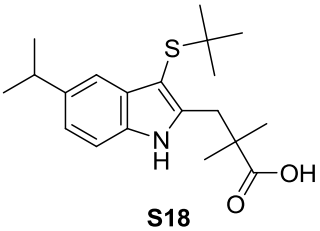
S18

[a] VH virtual hit from the screen with the partial query pharmacophore model

Chart S1. …continued.

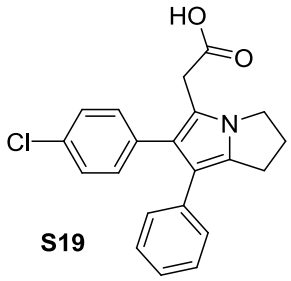

S19

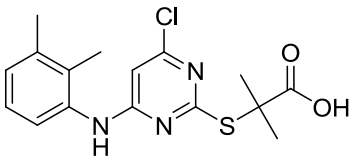

S20, VH[a]

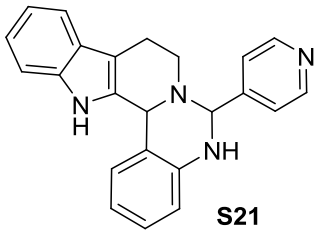

S21

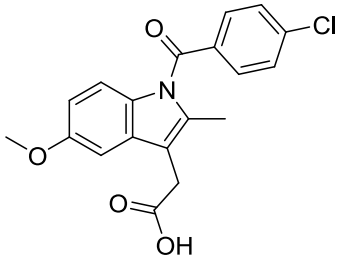

S22

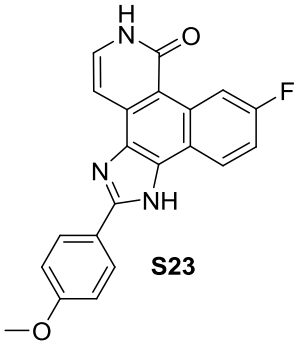

S23

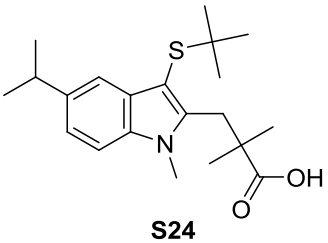

S24

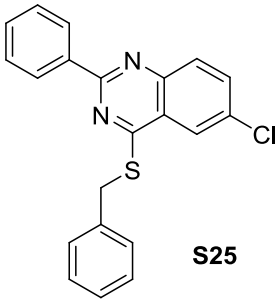

S25

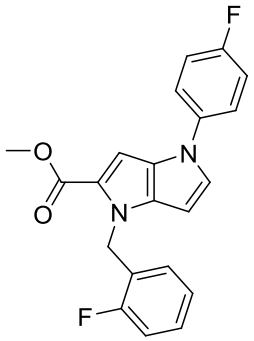

S26

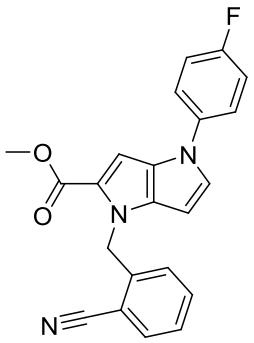

S27

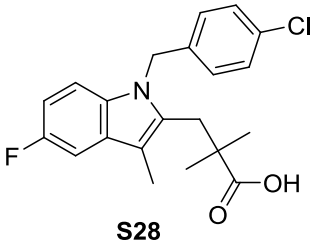

S28

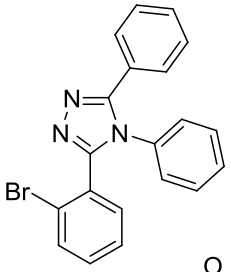

S29

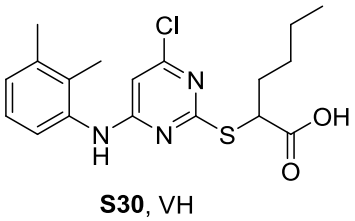

S30, VH

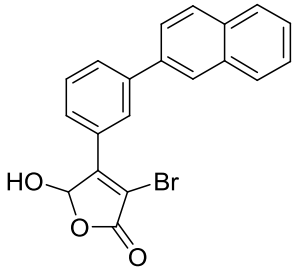

S31

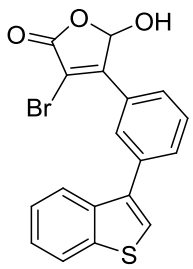

S32

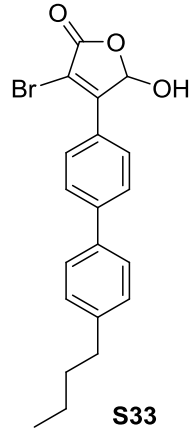

S33

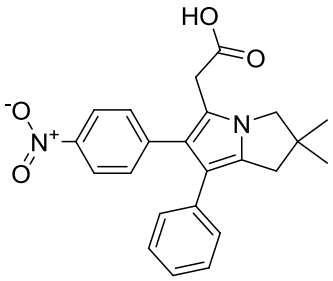

S34

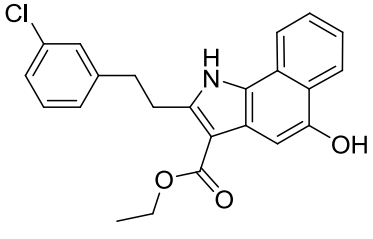

S35

[a] VH virtual hit from the screen with the partial query pharmacophore model

Chart S1. …continued.

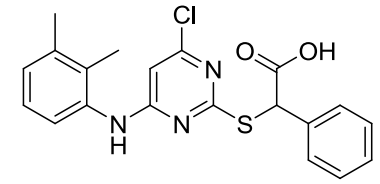

S36, VH[a]

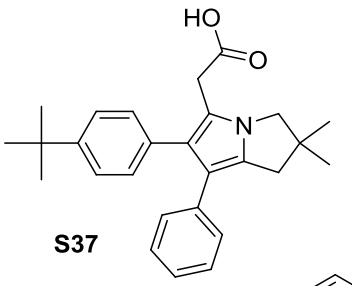

S37

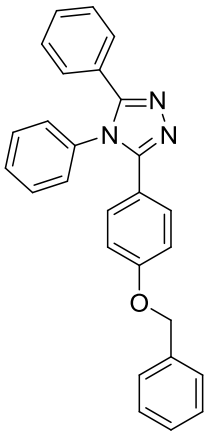

S38

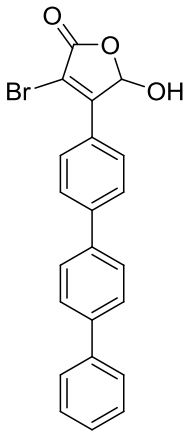

S39

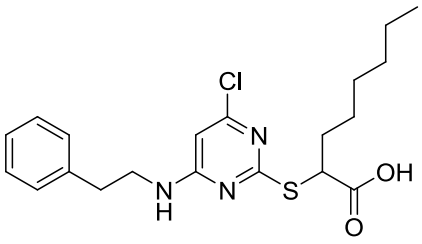

S40, VH

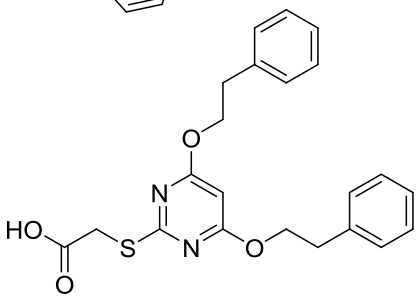

S41

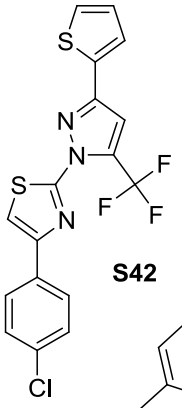

S42

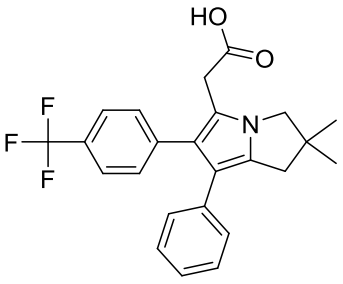

S43

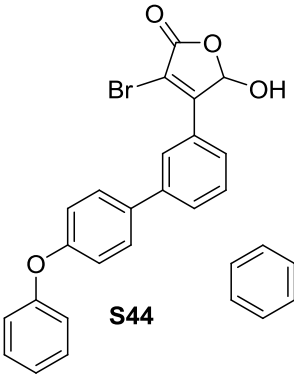

S44

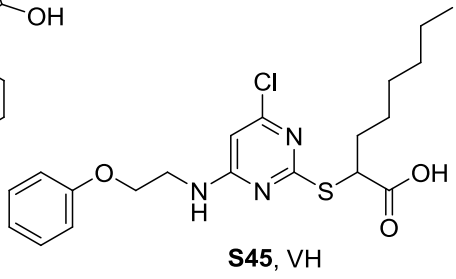

S45, VH

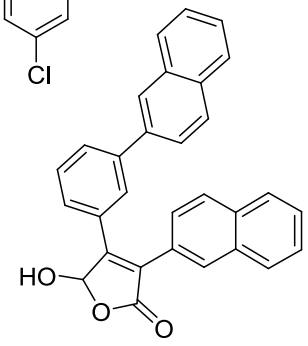

S46

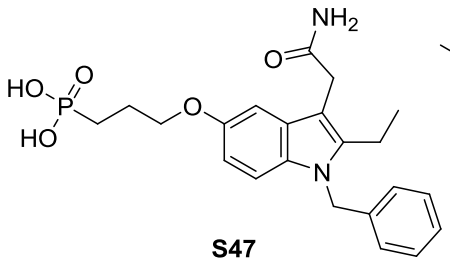

S47

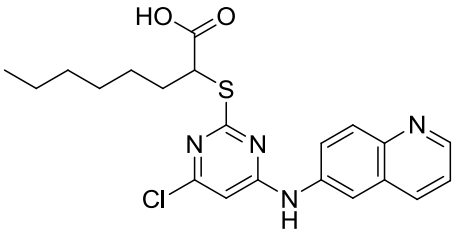

S48, VH

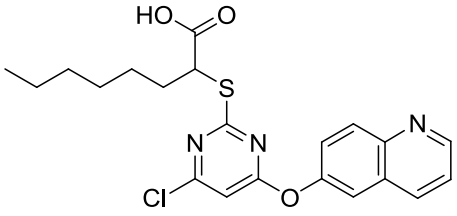

S49, VH

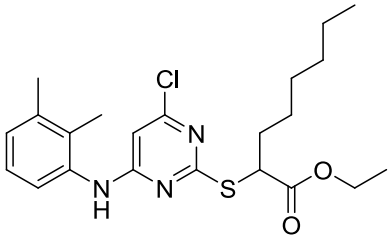

S50

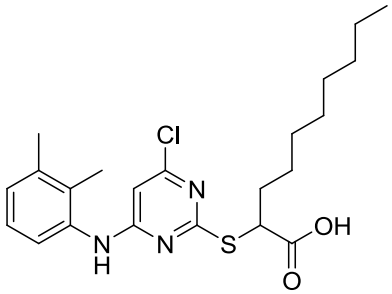

S51, VH

[a] VH virtual hit from the screen with the partial query pharmacophore model

Chart S1. …continued.

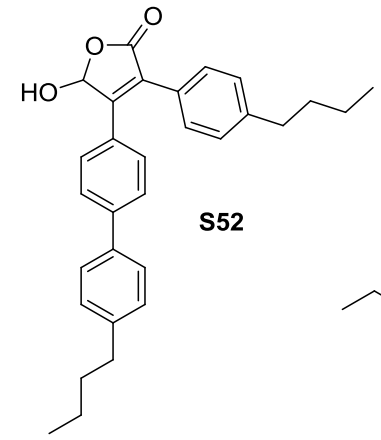

S52

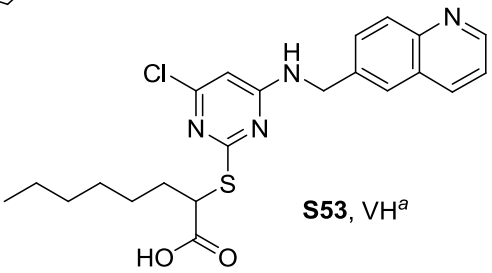

S53, VH[a]

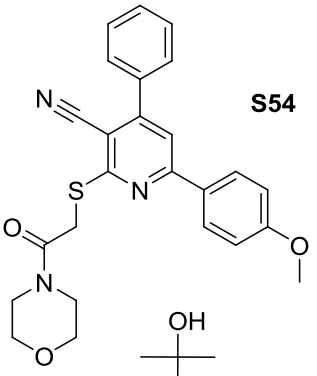

S54

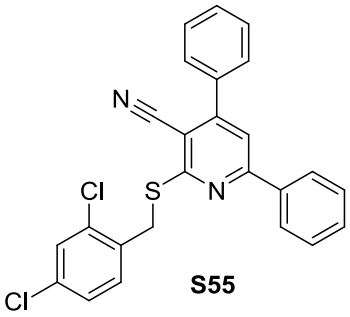

S55

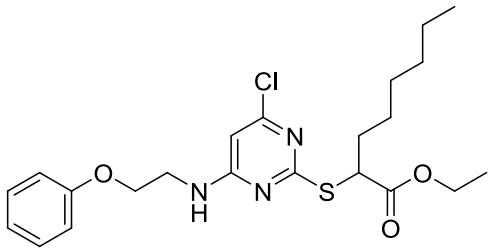

S56

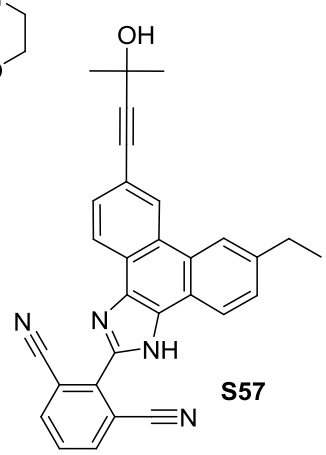

S57

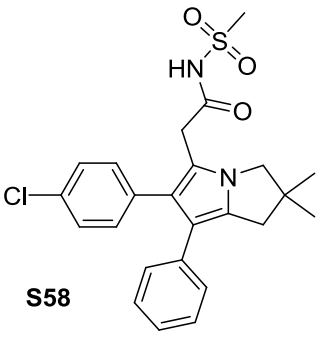

S58

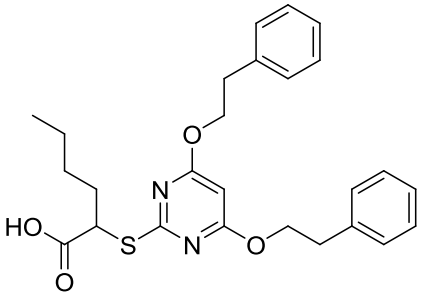

S59, VH

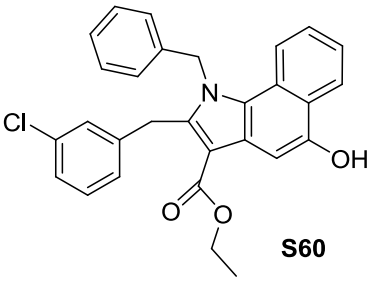

S60

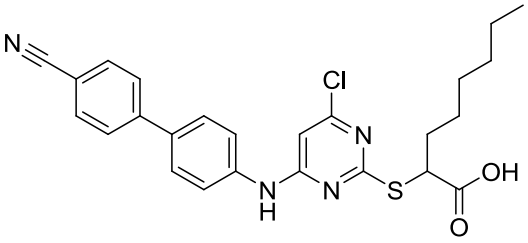

S61, VH

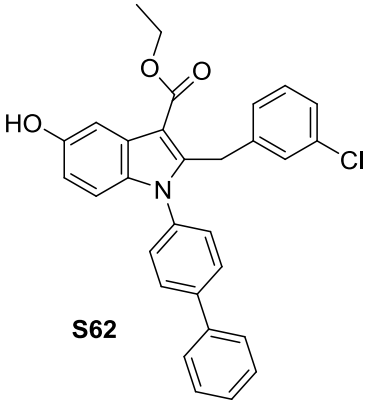

S62

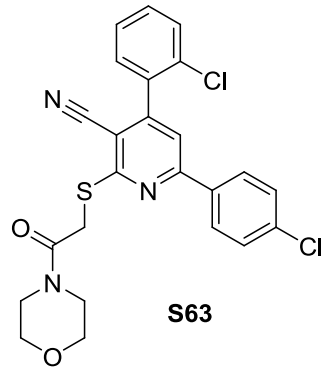

S63

[a] VH virtual hit from the screen with the partial query pharmacophore model

Chart S1. …continued.

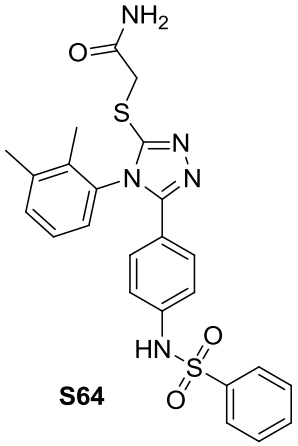

S64

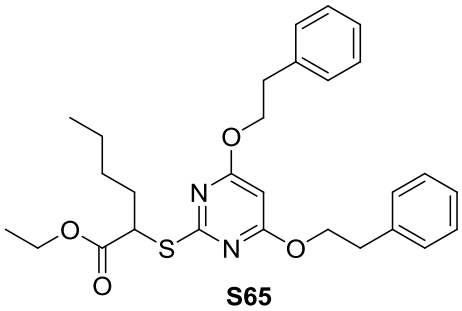

S65

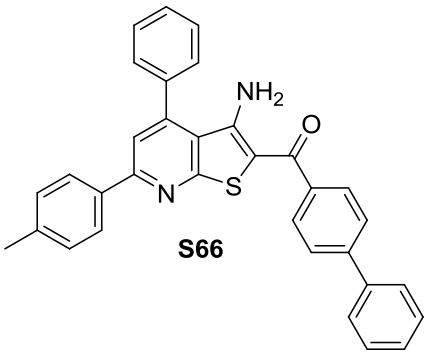

S66

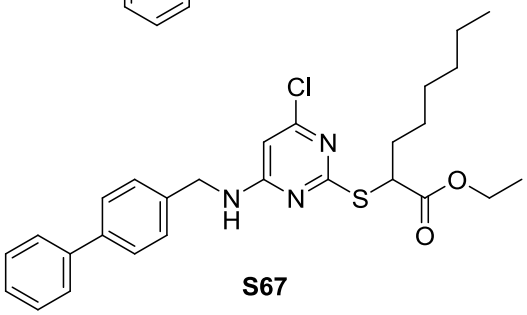

S67

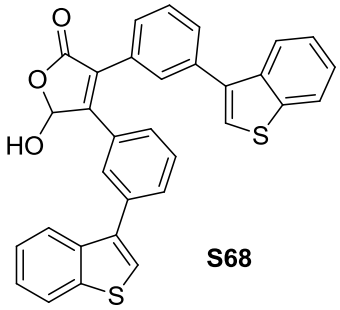

S68

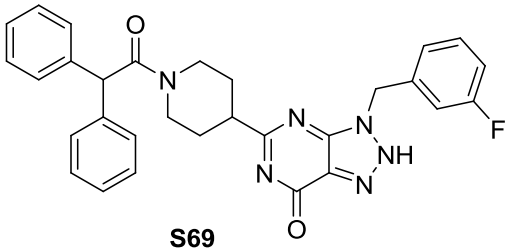

S69

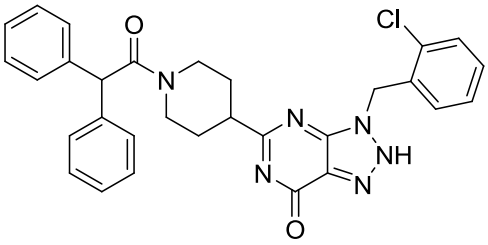

S70

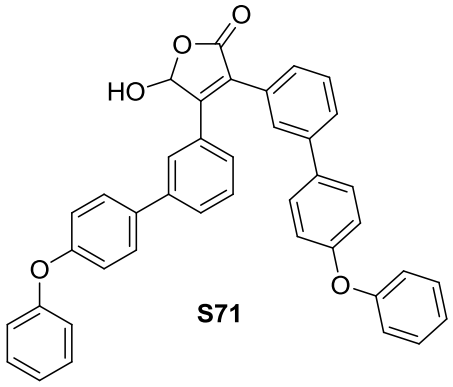

S71

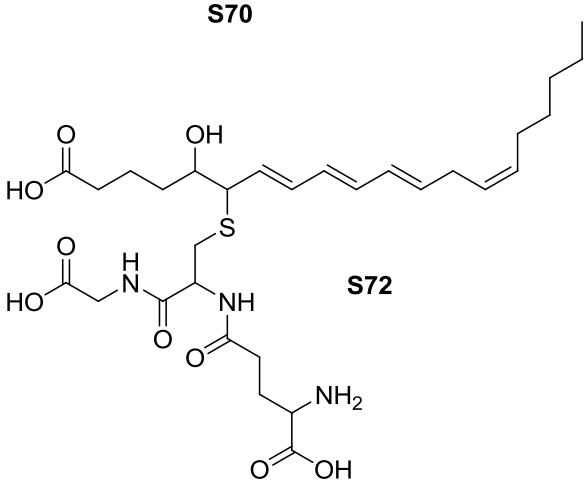

S72

Chart S2. Compounds from the NCI database mapping all six pharmacophore model features that were selected for biological testing.

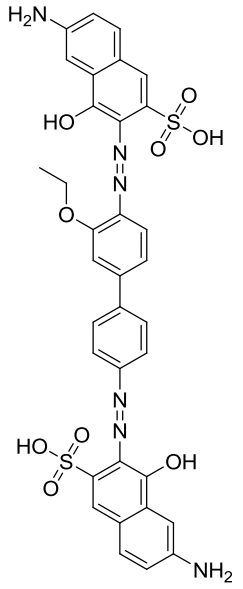

S73, ia[a]

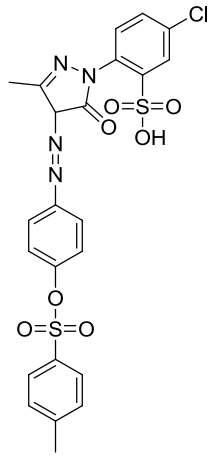

S74, ia

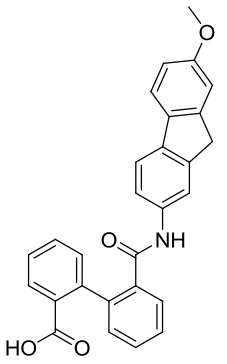

S75, ia

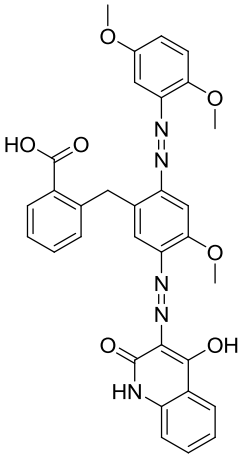

S76, nd[b]

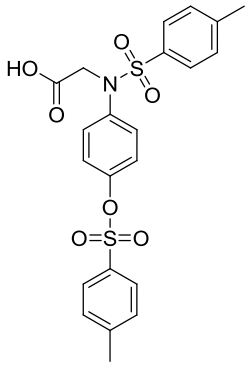

S77, ia

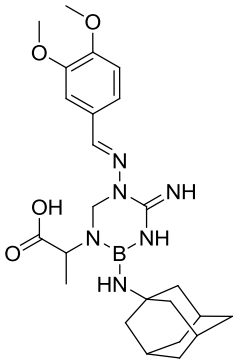

S78, ia

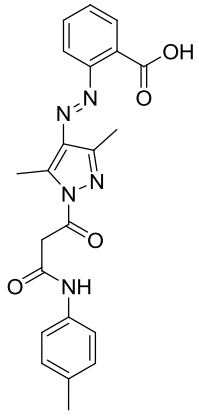

S79, ia

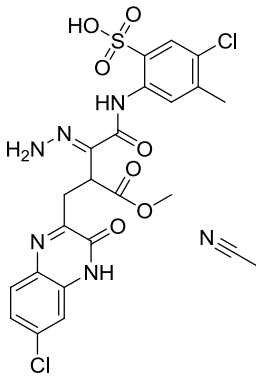

S80, ia

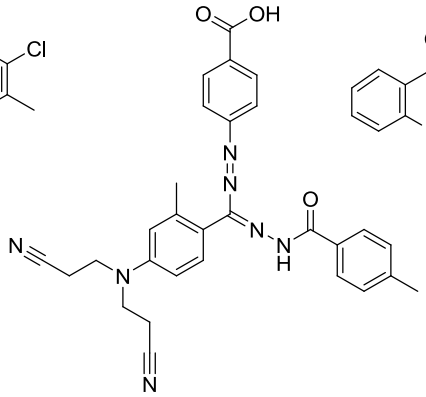

S81, nd

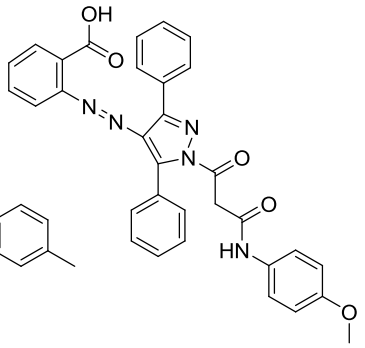

S82, ia

[a] ia inactive, [b] nd not determined (insoluble).

Chart S3. Compounds from the Specs database mapping all six pharmacophore model features that were selected for biological testing.

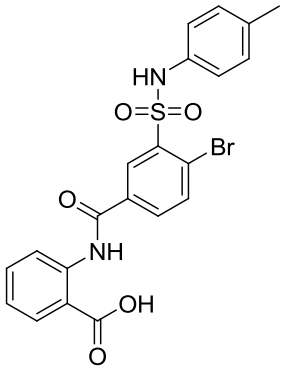

20

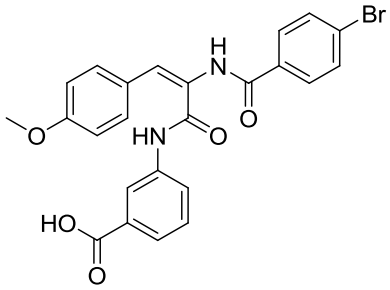

S83, ia[a]

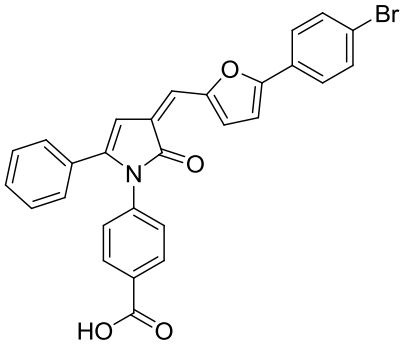

21

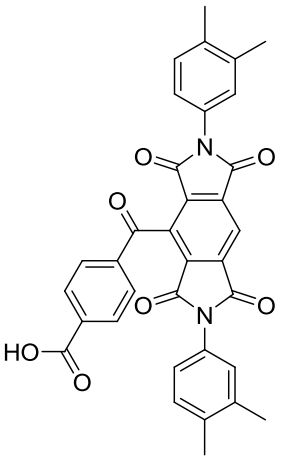

22

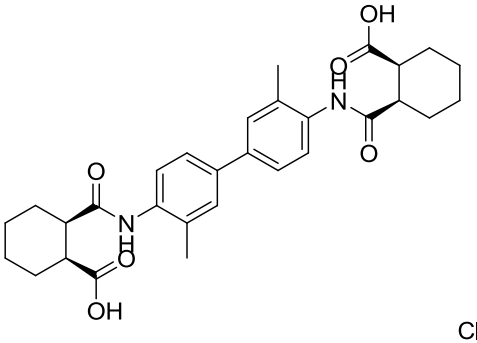

S84, ia

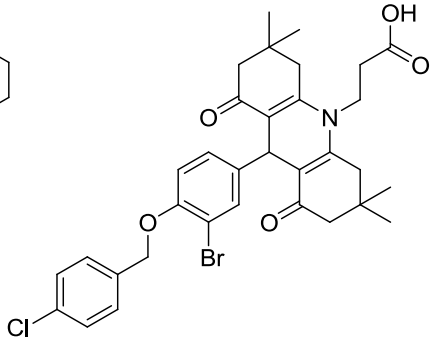

23

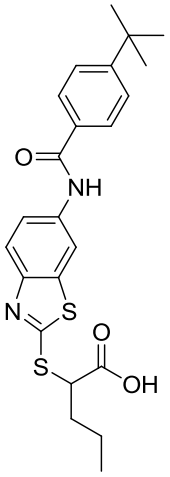

24

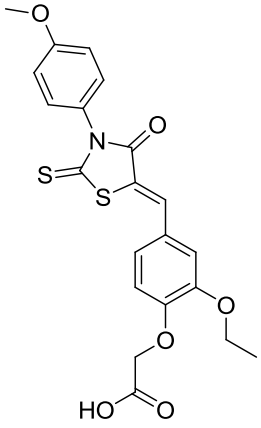

S85, ia

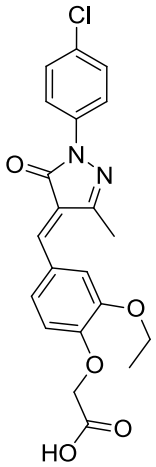

S86, ia

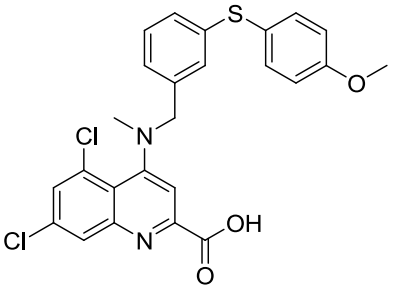

25

[a] ia inactive.

Chart S4. Compounds from the NCI database leaving out one pharmacophore model feature that were selected for biological testing.

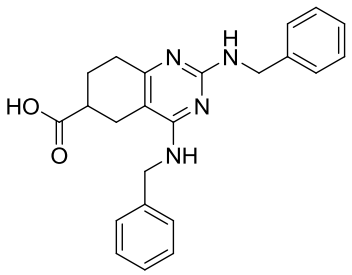

S87, ia[a]

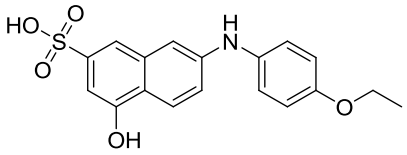

S88, ia

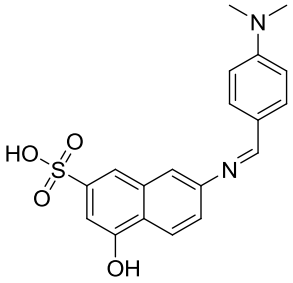

S89, nd[b]

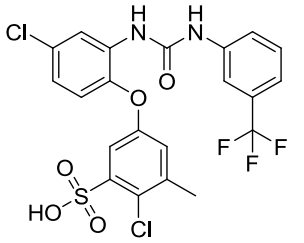

26

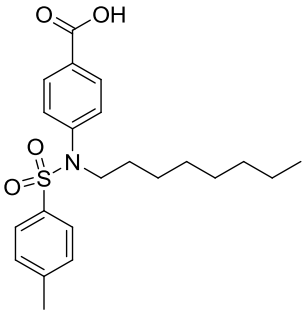

27

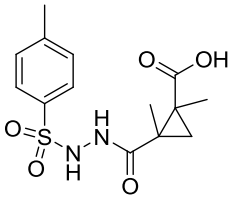

S90, nd

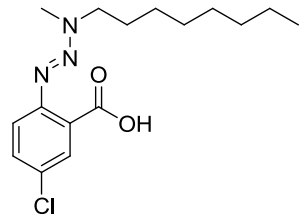

S91, ia

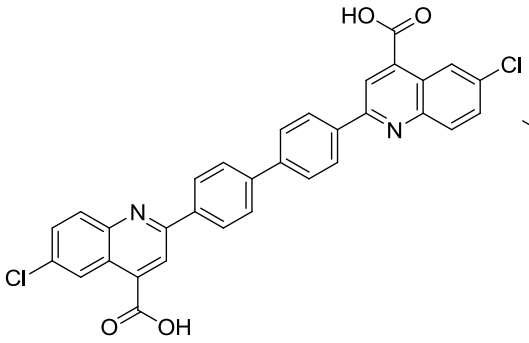

28

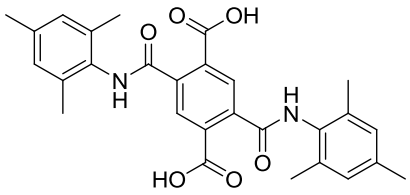

S92, ia

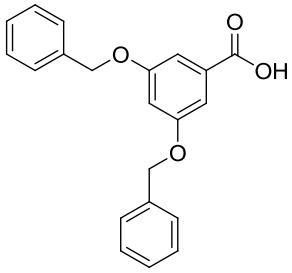

S93, ia

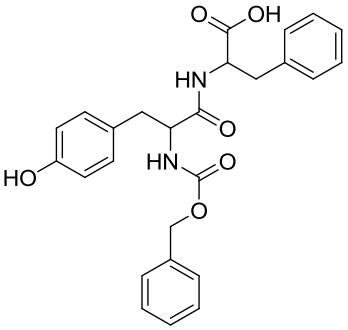

S94, ia

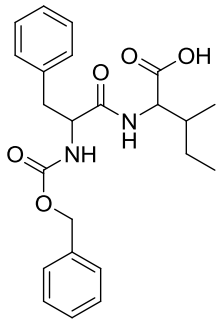

S95, ia

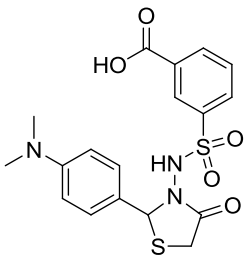

S96, ia

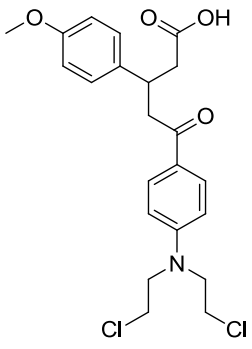

S97, nd

[a] ia inactive, [b] nd not determined (insoluble).

Chart S5. Structure of the 5-LO control inhibitor **S98** (BWA4C).

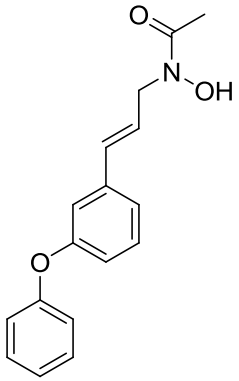

Figure S1. Cell viability given as mean ± S.E. A: Jurkat A3 cells, n = 4; B: A549 cells, n = 4. veh., vehicle (DMSO, 0.3%); CHX, cycloheximide, 50 µM; stsp., staurosporine, 3 µM.

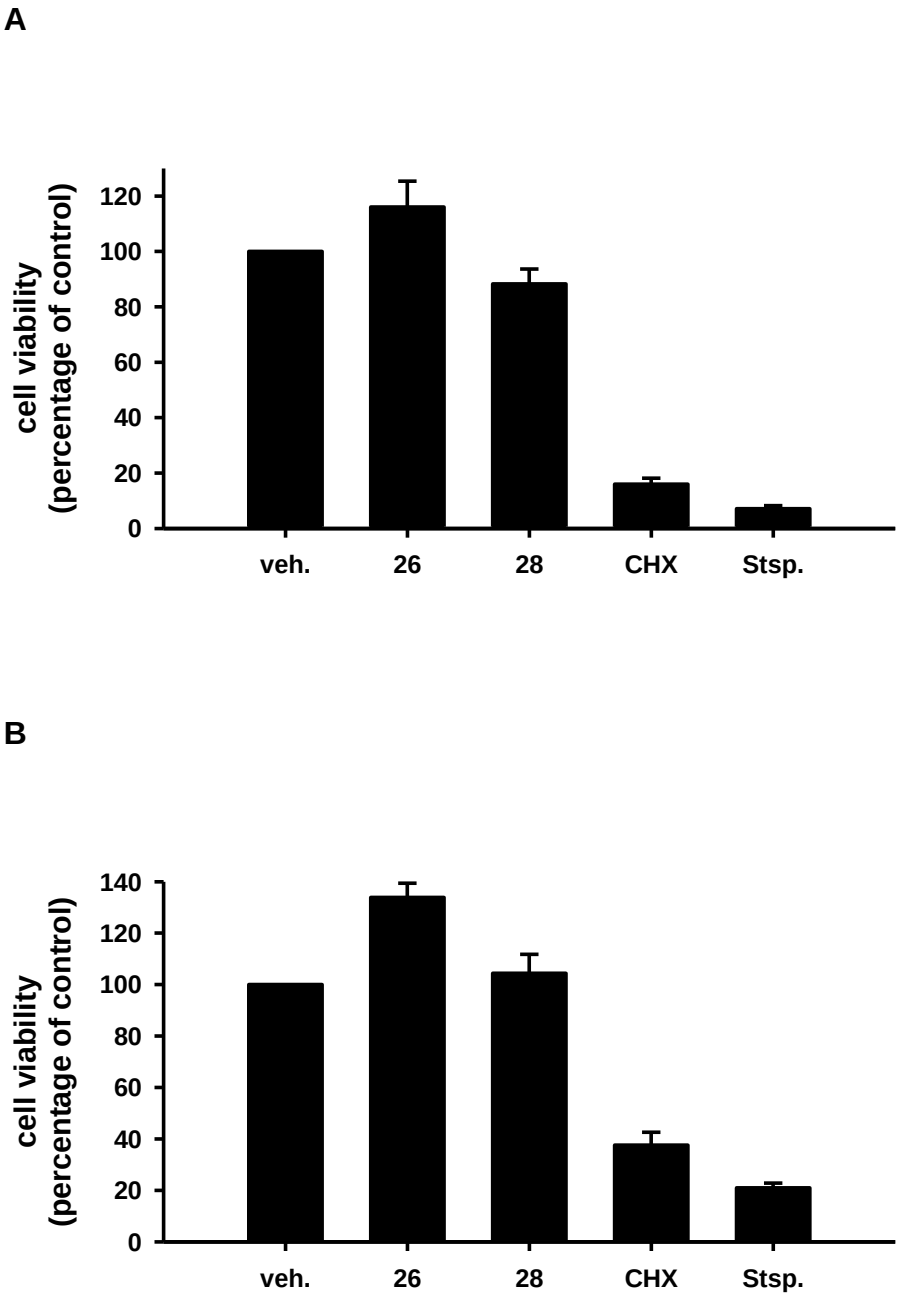

Molecular docking of mPGES-1 inhibitors

Worflow. The ligand-based pharmacophore model was developed using a dataset of acidic inhibitors of mPGES-1, and validated by means of screening a validation dataset composed of ligands and non-binders, referred to as inactives. In a quite similar way, the workflow of the molecular docking experiment was developed. Out of the 32 compounds reported by Riendeau et al.,[6] 12 compounds were selected and assigned to four activity classes: three classes of active ligands (n=9) and one class containing weakly active and inactive compounds (n=3, IC_{50} >10 µM)(Figure S2 and Table S1). The resulting four activity classes are from now on referred to as highly-actives (IC_{50} <100 nM), actives (IC_{50} 100 nM - 1 µM), moderately actives (IC_{50} 1 µM - 10 µM), and inactives (IC_{50} >10 µM). To suggest ligand binding poses of mPGES-1 inhibitors, including the inhibitors identified in this study, a molecular docking workflow in three steps was developed, consisting of protein and ligand preparation, molecular docking experiments, and scoring validation. For this purpose, the molecular modeling suite Maestro was applied, as well as the software tool analyse-it for the statistical evaluation.[9, 10] The development of the workflow was performed by conducting the induced-fit docking (IFD) workflow in Maestro with different settings. Afterwards, the IFD run with the best settings was identified out of several docking runs, by evaluating the consistency of the predictions with the experimental data. In the first step of the validation, the activity class predicted by docking and scoring was compared to the *in vitro* activity class. Thereby, the ranking power of the approach was assessed. In the second step, the Pearson's correlation coefficient (R_P) of the docking scores and the pIC_{50}-values of the ligands was investigated, which is referred to as evaluation of the scoring power.[11, 12]

Figure S2. Compounds that were used for validating the docking run along with compounds **5** (highly active), **9** (moderately active), **S18**, and **S24** (both inactive).

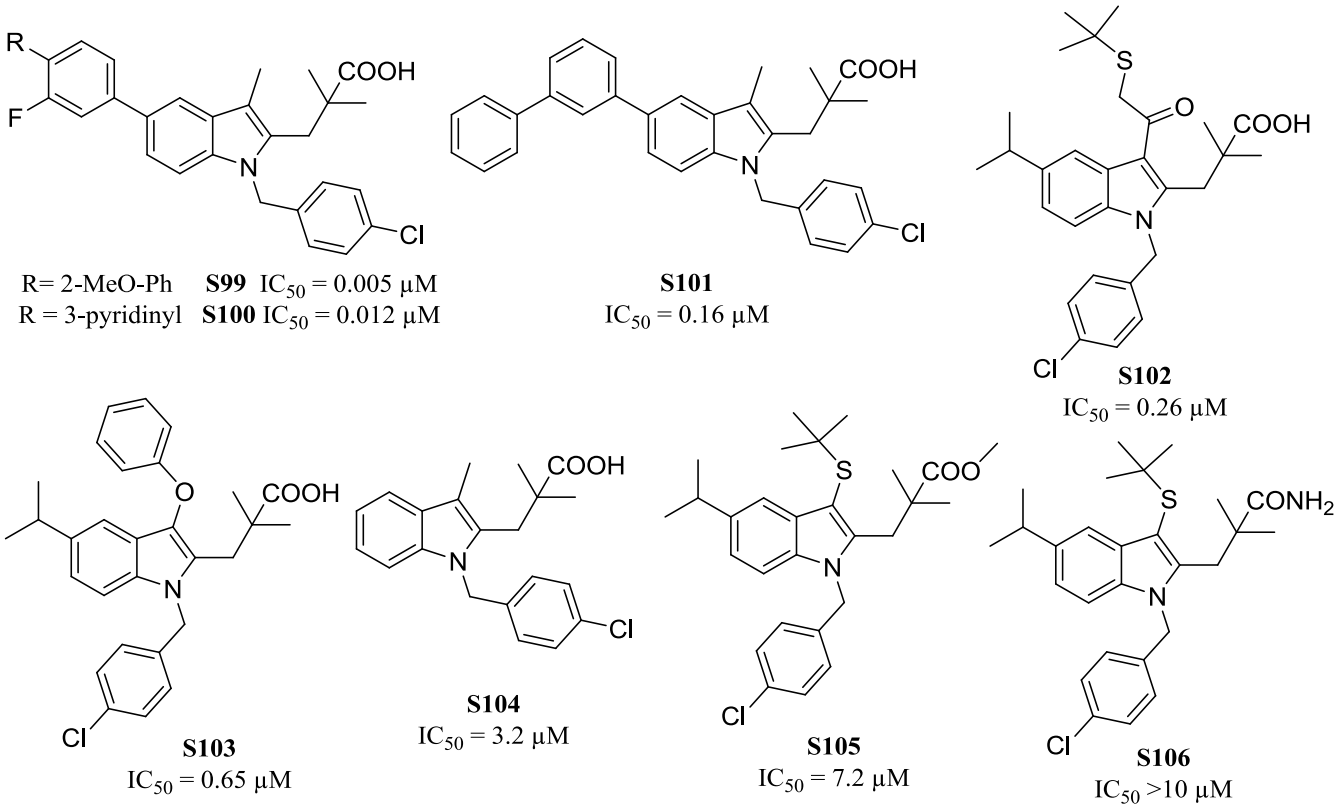

1.2 Ligand Preparation

The 2D representations of all compounds that were submitted to the molecular docking experiment were converted to 3D coordinates using the Ligprep module in Maestro. Afterwards, the geometry optimization and the calculation of atomic partial charges were conducted by means of using the unrestricted Hartree-Fock (unrestricted HF/UHF) method for the calculations, which represents a calculation method based upon QM theory.[13] In the first step of the computations, the geometry of all compounds was optimized using the HF/6-31G level of QM calculations. In the second step, the atomic partial charges of all compounds were calculated using the HF/6-311G* calculation level, again in the spin-unrestricted mode, classified among the HF methods as the UHF method. These computations that were required for the preparation of all compounds prior to the molecular docking were performed using the Jaguar module in Maestro with the level of the iterative energy minimization assigned to accurate. These methods are described and extensively cited in the Jaguar manual.

1.3 Protein Preparation

The electron crystallographic structure of mPGES-1 (PDB code 3dww) was preprocessed in Maestro by adding hydrogen atoms and calculating charges.[14] Afterwards, the protein was submitted to an exhaustive optimization of the hydrogen bond assignment, allowing a rearrangement of hydroxyl groups, side chain amide moieties, and histidine side chain protonation states. Finally, the protein was minimized by applying the OPLS 2001 force field implemented in Maestro using a RMSD threshold of 0.18 Å.

1.4 Induced-fit Docking (IFD)

The docking experiment was conducted using the IFD protocol in Maestro, which applies a hybrid approach consisting of soft receptor docking, employment of side chain rotamere libraries, and optionally involving mutational alanine replacement of bulky side chains.[15] The binding site required for the docking experiment into the homotrimeric protein was assigned at the interface of helix 4 of subunit A and helix 1 of subunit B, accounting to the hypothesis that the inhibitor binding site is located in similar regions within members of the MAPEG family.[16] The central residue Tyr28 of this interface was assigned the center for the IFD protocol, and the bulky side chains of the residues Tyr28, Ile32, and Gln134 were replaced by alanine in the initial Glide-docking. Afterwards, the residues in a range of 5 Å within the initial ligand binding poses were re-positioned in the Prime-refinement that was performed as second step in the IFD protocol. In the third step, the resulting macromolecule geometries were used for the second Glide-docking without receptor vdWaals radius scaling and with the original side chain moieties reconstituted. For this step in the IFD protocol, as in the first step, the Glide-docking was performed in Glide-SP mode.[17]

1.5 Validation

The molecular docking experiment was conducted in the first run by placing the compounds in the putative binding site that included the cofactor GSH. In the second run, the cofactor was removed prior to the optimization of the 3D structure. In brief, the results of the first run were not found to be significant (data not shown), while the results retrieved in the second run indicate that the discriminatory capability of the IFD workflow is robust. In the second run, all nine ligands were successfully docked, as well as two out of three inactives. In detail, all highly-actives were given a high rank, all actives and moderately actives were placed in the correct group or the neighbor group. In addition, one out of the three inactive compounds was not docked, thus rejected correctly. The other two inactive compounds were placed in the binding site. One of these inactive compounds was given a

medium rank. This is the only compound that was not classified in the correct or neighboring activity group (Table S1). Furthermore, the scoring power was determined for the results of the protein-ligand docking, accounting the highest score achieved by each ligand in the second docking run (Figure S3). The scoring function of Glide, applied in the reported IFD workflow, attained a Pearson's correlation coefficient of 0.86 (R_P^2 = 0.74) between the Glide-score and the pIC_{50}-values of all ligands included in the validation of the IFD workflow. In summary, the results showed that the presented IFD workflow, validated by investigating the consistency of the predictions with the experimental data, represents a valid approach for the prediction of the ligand binding poses of the novel chemical classes of inhibitors identified in this study.

Table S1. The Glide-scores for all ligands and inactives are given, placing the compound into one of four activity classes. This predicted activity class is compared to the activity class derived from experimental data, to evaluate the consistency of the predictions with the experimental data.

Entry ID	Glide gscore	pIC_{50}	activity class (*in vitro*)	activity class (predicted)
S99	-14.65	8.3	+++	+++
S100	-11.43	7.92	+++	+++
5	-13.60	7.8	+++	+++
S101	-12.58	6.8	++	+++
S102	-8.15	6.58	++	++
S103	-4.54	6.19	++	+
S104	-8.52	5.49	+	++
9	-6.02	5.17	+	+
S105	-4.86	5.14	+	+
S106	-5.04	<5	-	+
S18	-9.74	<5	-	++
S24	-	<5	-	-

Figure S3. 2D graph showing the correlation by plotting the Glide-scores against the pIC_{50}-values of the ligands.

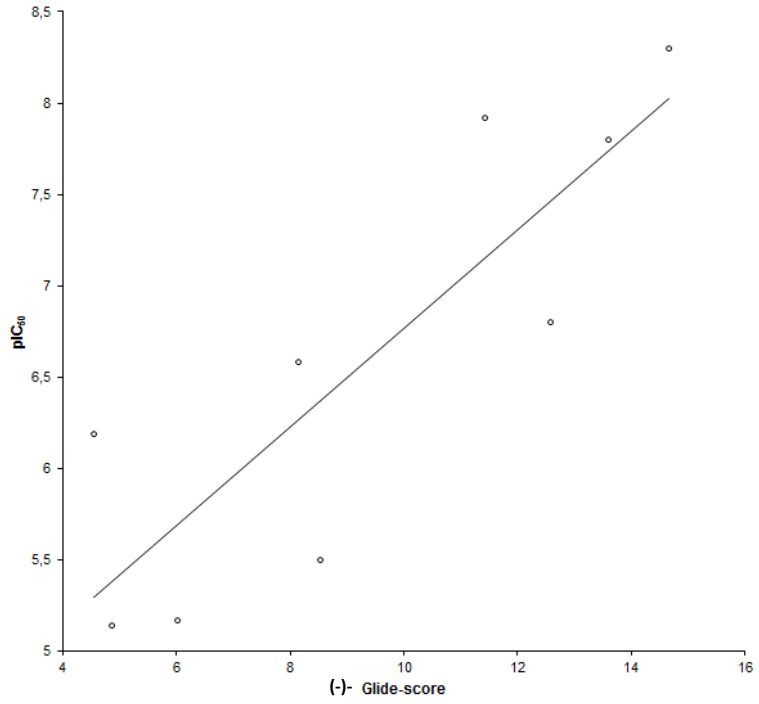

Supporting Information References

1. Edwards, B. S.; Bologa, C.; Young, S. M.; Balakin, K. V.; Prossnitz, E. R.; Savchuck, N. P.; Sklar, L. A.; Oprea, T. I. Integration of virtual screening with high-throughput flow cytometry to identify novel small molecule formylpeptide receptor antagonists. *Mol. Pharmacol.* 2005, 68, (5), 1301-1310.

2. Friesen, R. W.; Mancini, J. A. Microsomal prostaglandin E2 synthase-1 (mPGES-1): a novel anti-inflammatory therapeutic target. *J. Med. Chem.* 2008, 51, (14), 4059-67.

3. Koeberle, A.; Zettl, H.; Greiner, C.; Wurglics, M.; Schubert-Zsilavecz, M.; Werz, O. Pirinixic acid derivatives as novel dual inhibitors of microsomal prostaglandin E2 synthase-1 and 5-lipoxygenase. *J. Med. Chem.* 2008, 51, (24), 8068-76.

4. Olofsson, K.; Suna, A.; Pelcman, B.; Ozola, V.; Katkevics, M.; Kalvins, I.; Schaal, W. Indoles useful in the treatment of inflammation. Int. Pat. Appl. PCT WO 2005/123675 A1, 29.12., 2005.

5. Olofsson, K.; Suna, A.; Pelcman, B.; Ozola, V.; Katkevics, M.; Kalvins, I. Indoles useful for the treatment of inflammation. Int. Pat. Appl. PCT WO 2005/123673 A1, 29.12., 2005.

6. Riendeau, D.; Aspiotis, R.; Ethier, D.; Gareau, Y.; Grimm, E. L.; Guay, J.; Guiral, S.; Juteau, H.; Mancini, J. A.; Methot, N.; Rubin, J.; Friesen, R. W. Inhibitors of the inducible microsomal prostaglandin E2 synthase (mPGES-1) derived from MK-886. *Bioorg. Med. Chem. Lett.* 2005, 15, (14), 3352-5.

7. Rohrer, S. G.; Baumann, K. Maximum unbiased validation (MUV) data sets for virtual screening based on PubChem bioactivity data. *J. Chem. Inf. Model.* 2009, 49, (2), 169-184.

8. Rorsch, F.; Wobst, I.; Zettl, H.; Schubert-Zsilavecz, M.; Grosch, S.; Geisslinger, G.; Schneider, G.; Proschak, E. Nonacidic inhibitors of human microsomal prostaglandin synthase 1 (mPGES 1) identified by a multistep virtual screening protocol. *J. Med. Chem.* 2010, 53, (2), 911-5.

9. Maestro Suite, version 8.5. *Schrödinger, LLC* 2008.

10. Analyse-it for MS Excel (version 2.20). *Analys-it Software, Ltd.* http://www.analyse-it.com/ 2009.

11. Cheng, T.; Li, X.; Li, Y.; Liu, Z.; Wang, R. Comparative assessment of scoring functions on a diverse test set. *J Chem Inf Model* 2009, 49, (4), 1079-1093.

12. Seifert, M. H.; Kraus, J.; Kramer, B. Virtual high-throughput screening of molecular databases. *Curr Opin Drug Discov Devel* 2007, 10, (3), 298-307.

13. Gleeson, M. P.; Gleeson, D. QM/MM as a tool in fragment based drug discovery. A cross-docking, rescoring study of kinase inhibitors. *J Chem Inf Model* 2009, 49, (6), 1437-1448.

14. Jegerschold, C.; Pawelzik, S. C.; Purhonen, P.; Bhakat, P.; Gheorghe, K. R.; Gyobu, N.; Mitsuoka, K.; Morgenstern, R.; Jakobsson, P. J.; Hebert, H. Structural basis for induced formation of the inflammatory mediator prostaglandin E2. *Proc. Natl. Acad. Sci. U.S.A.* 2008, 105, (32), 11110-5.

15. B-Rao, C.; Subramanian, J.; Sharma, S. D. Managing protein flexibility in docking and its applications. *Drug Discov. Today* 2009, 14, (7/8), 394-400.

16. Pawelzik, S. C.; Uda, N. R.; Spahiu, L.; Jegerschold, C.; Stenberg, P.; Hebert, H.; Morgenstern, R.; Jakobsson, P. J. Identification of key residues determining species differences in inhibitor binding of microsomal prostaglandin E synthase-1. *J Biol Chem* 2010, 285, (38), 29254-61.

17. Sherman, W.; Day, T.; Jacobson, M. P.; Friesner, R. A.; Farid, R. Novel procedure for modeling ligand/receptor induced fit effects. *J Med Chem* 2006, 49, (2), 534-53.